ELSEVIER

Clinical Neurophysiology 115 (2004) 710–720

www.elsevier.com/locate/clinph

Effects of electrode density and electrolyte spreading in dense array electroencephalographic recording

Lawrence L. Greischar[a,b,*], Cory A. Burghy[a], Carien M. van Reekum[a], Daren C. Jackson[a], Diego A. Pizzagalli[c], Corrina Mueller[a], Richard J. Davidson[a,b]

[a]*Department of Psychology, University of Wisconsin–Madison, Brogden Hall, Room 371, 1202 West Johnson Street, Madison, WI 53706, USA*
[b]*W.M. Keck Laboratory for Functional Brain Imaging and Behavior, University of Wisconsin–Madison, 1500 Highland Avenue, Madison, WI 53705, USA*
[c]*Department of Psychology, Harvard University, 33 Kirkland Street, Cambridge, MA 02138, USA*

Accepted 23 October 2003

Abstract

Objective: High-density EEG recording offers increased spatial resolution but requires careful consideration of how the density of electrodes affects the potentials being measured. Power differences as a function of electrode density and electrolyte spreading were examined and a method for correcting these differences was tested.

Methods: Separate EEG recordings from 8 participants were made using a high-density electrode net, first with 6 of 128 electrodes active followed by recordings with all electrodes active. For a subset of 4 participants measurements were counterbalanced with recordings made in the reversed order by drying the hair after the high-density recordings and using a fresh dry electrode net of the same size for the low-density recordings. Mean power values over 6 resting eyes open/closed EEG recordings at the 6 active electrodes common to both recording conditions were compared. Evidence for possible electrolyte spreading or bridging between electrodes was acquired by computing Hjorth electrical distances. Spherical spline interpolation was tested for correcting power values at electrodes affected by electrolyte spreading for these participants and for a subset of participants from a larger previous study.

Results: For both the complete set and the counterbalanced subset, significant decreases in power at the 6 common electrodes for the high-density recordings were observed across the range of the standard EEG bands (1–44 Hz). The number of bridges or amount of electrolyte spreading towards the reference electrode as evidenced by small Hjorth electrical distances served as a predictor of this power decrease. Spherical spline interpolation increased the power values at electrodes affected by electrolyte spreading and by a significant amount for the larger number of participants in the second group.

Conclusions: Understanding signal effects caused by closely spaced electrodes, detecting electrolyte spreading and correcting its effects are important considerations for high-density EEG recordings. A combination of scalp maps of power density and plots of small Hjorth electrical distances can be used to identify electrodes affected by electrolyte spreading. Interpolation using spherical splines offers a method for correcting the potentials measured at these electrodes.

Keywords: Electroencephalography; Electrolyte spreading; Dense array

1. Introduction

Adequate spatial sampling of scalp electrical potentials is necessary for optimal resolution of the sources within the brain (Tucker, 1993; Srinivasan et al., 1998; Lantz et al., 2003). In recent years new solutions for high-density EEG recording have been implemented but have been slow to come into general use due to the difficulty of applying large numbers of electrodes particularly when scalp abrasion is required, the increased possibility for electrolyte spreading or bridging of the shorter distances between electrodes, and the greatly increased data processing requirements often involving artifact scoring by humans. One solution, the128-channel geodetic sensor net, (GSN128; Electrical Geodesics Inc., Eugene, OR) offers relatively quick and easy application without the need for scalp abrasion (Ferree and Tucker, 1999; Ferree et al., 2001). However, the risk of electrolyte spreading and increased processing requirements remain.

* Corresponding author. Tel.: +1-608-262-9944; fax: +1-608-265-2875.
E-mail address: greischar@psyphw.psych.wisc.edu (L.L. Greischar).

1388-2457/$30.00
doi:10.1016/j.clinph.2003.10.028

A GSN128 electrode consists of an Ag/AgCl pellet in contact with a saline (KCl) soaked sponge encased in a flared plastic pedestal designed to keep the saline electrolyte in contact with the scalp and shield it from being wicked away by strands of hair. These electrode pedestals are arranged in a geodetic structure (see Tucker, 1993 for details) using slightly elastic monofilament line so that the tension tends to push them vertically down onto the scalp. Opportunities for electrolyte spreading occur during initial positioning of electrodes on the scalp and subsequent wiggling of individual electrode pedestals in order to obtain good scalp contact with sufficiently low electrode impedances. Electrolyte drying or additional spreading due to wicking by hair could potentially change electrolyte spreading effects during EEG recordings.

Comparisons of low- and high-density EEG recordings have been primarily concerned with the spatial resolution of electrical sources in the brain (Spitzer et al., 1989; Tucker, 1993; Srinivasan et al., 1998) while the effects that large numbers of highly conductive electrodes and associated electrolyte have on potentials measured on the scalp surface boundary have been largely ignored. However, one direct comparison of ERPs recorded at high density using the GSN128 and a conventional 30-channel system (Electro-Cap International Inc.) was made by Kayser et al. (2000). Their results for ERPs averaged over 17 subjects with both 30- and 128-channel data showed smaller ERP amplitudes and lower signal-to-noise ratios for the 128-channel data which could be related to electrode density and electrolyte spreading. Since our EEG work is largely concerned with estimating parameters of brain electrical asymmetry (Davidson, 1988; Tomarken et al., 1992) we set out to perform a similar comparison of low- and high-density EEG recordings in order to assess the effects on electrode power estimates due to increased electrode density and possible effects (especially asymmetrical ones) of electrolyte spreading. Computation of asymmetrical brain electrical measures involves power estimates from a participant during a single recording session so that possible asymmetrical effects of electrolyte spreading are not removed by averaging. Initial analyses of frontal asymmetry scores from a study which used EEG data collected with the high-density GSN128 indicated that overall test-retest stability (alpha 8–13 Hz F3/4, average mastoid reference, $r = 0.22$, $n = 150$, $P = 0.007$) was significantly lower than that of a comparable low-density study (alpha 8–13 Hz F3/4, average ears reference, $r = 0.66$, $n = 85$, $P = 0.001$; Tomarken et al., 1992) (Fisher's test for independent correlations: $Z = -4.13$, $P < 0.0001$; Fisher, 1921). In addition, male participant's test-retest stability (alpha 8–13 Hz F3/4, average mastoid reference $r = 0.56$, $n = 18$, $P = 0.017$) was higher than for females (alpha 8–13 Hz F3/4, average mastoid reference $r = 0.22$, $n = 132$, $P = 0.013$) (Fisher's test for independent correlations: $Z = 1.50$, $P < 0.14$; Fisher, 1921), suggesting that hair length might be a factor.

A simple experiment was run to test directly for power differences between low- and high-density EEG recordings. The GSN128 was first applied with only 6 electrodes soaked in electrolyte and active, resting recordings were made, and the net was removed and reapplied with all electrodes soaked in electrolyte and active. A second set of resting recordings was made, and power densities were compared between conditions for the original 6 active electrodes. For a subset of the participants recordings were made in reversed order (128 followed by 6 active electrodes) to verify that results were not affected by the order in which the recordings were made. For the high electrode density portion of the reversed order recordings the recently released on-line bridge detection software (Electrical Geodesics Inc., 2003) was tested for comparison with the off-line method described in this paper.

In order to detect electrolyte spreading or bridging Hjorth electrical distances were computed off-line using the method suggested in Tenke and Kayser (2001). The Hjorth electrical distance between two electrodes is simply the temporal variance of their difference potential, which would be decreased by electrolyte spreading or bridging between them. Thus anomalously small Hjorth electrical distances could indicate electrolyte spreading or bridging and a series of them between an electrode and the reference electrode could be the source of a power decrease at that electrode. Such an effect would seriously compromise an asymmetry score based on homologous electrodes where the power at one site was affected more than its homologous site by electrolyte spreading for the duration of all resting EEG recordings.

A practical solution to power changes associated with electrolyte spreading was examined and a second experiment was performed to extend the method to a different data set with more participants. A subset of 17 participants from a large study of EEG asymmetry was selected based on a moderate number of small Hjorth electrical distances in the left frontal area where power decrements could potentially affect frontal asymmetry scores. It was predicted that interpolation of voltages at the affected electrodes using values from the remaining unaffected electrodes would significantly change their powers. Given the importance of variations in alpha power for the assessment of regional activations associated with cognitive (e.g. Davidson et al., 1990) and affective (see e.g. Davidson et al., 2000a, for review) processes, log-transformed power density in the alpha band was examined.

2. Methods

2.1. Participants

Eight individuals (4 female) with ages ranging from 23 to 53 (mean = 33, SD = 9) volunteered to participate after giving informed consent. All participants were treated in accordance with institutional guidelines.

In view of the fact that our earlier work with high-density EEG recordings using the GSN128 had suggested that hair length might be a factor in electrolyte spreading the following description is given. Three of the male participants had full heads of generally straight non-thinning hair ranging in length from about 3 to 8 cm (participants 7, 6, and 3 ordered from short to long) and one male was bald on top and front with about 2 cm hair length on the sides (participant 2). Participant 3's hair was cut between the original and reversed order recordings changing it from a relatively long lay-over style to a much shorter (~3 cm) radial pattern. One of the female participants had hair about 5 cm above shoulder level (participant 8), two had approximately shoulder-length hair (participants 4 and 5) and one had hair extending to mid-back level (participant 1). Participants 1 and 8 had straight hair while participants 4 and 5 had denser and curlier hair textures.

2.2. Procedure

Six 1 min eyes open/closed resting EEG recordings, using a randomly assigned counterbalanced order (see Tomarken et al., 1992 for details), were collected using the normal and a novel method of applying the GSN128. Technicians with over a year's experience in the normal use of the GSN128 applied the electrode nets. The novel application method resulted in EEG recordings from 6 sites referenced to Cz. Each of the 6 electrodes (GSN128 numbers 24, 3, 37, 105, 60, 86), as well as the recording reference Cz and ground (located just above the nasion) were individually soaked in electrolyte prior to net application with the remaining 122 left dry and without effective electrical contact to the scalp. These 6 active electrodes correspond respectively to AF3/4, C3/4, PO3/4 in the International 10–10 reference system (Luu and Ferree, 2000). After completing the first set of recordings the GSN128 was removed from the participant's head and reapplied using the standard application procedure (EGI System 200 Technical Manual) with all electrodes soaked for about 1 min in electrolyte followed by excess electrolyte removal by patting the electrode sponges with a dry towel. These two methods of applying the GSN128 will be referred to as the low-density (LD: 6 active electrode) condition and high-density (HD: 128 active electrode) condition.

In order to test whether the observed effects were due the LD/HD ordering of the measurements, recordings were made in the reversed HD/LD order for 4 of the participants by using two different GSNs and blow drying hair between recordings sessions. For 3 of these participants a pair of medium-sized GSN128s were used with counterbalanced order between HD and LD recordings, and for the 4th a pair of large sized GSN128s were used. Also at this time the recently released on-line electrolyte bridge detection feature (Electrical Geodesics Inc., 2003) of Netstation 3.0 was tested. Immediately after impedances were measured this program was run and bridged electrodes (using the default threshold of 1 μV^2) were listed in the recording notes. No attempt was made to fix bridged electrodes since a comparison of these with the off-line results was desired.

Following recommended procedures, the electrolyte used to soak the GSN128 sponge electrodes consisted of 1.5 teaspoons (~8.5 g) of potassium chloride and a few drops of baby shampoo in one liter of distilled water (EGI System 200 Technical Manual).

EEG was recorded using EGI amplifiers and Netstation version 2.0 software (version 3.0 with on-line bridge detection feature for HD/LD recordings). Signals were sampled at 250 Hz with 16 bit precision. Hardware filters were set at 0.1 and 100 Hz. Amplifier gains and zeros were measured prior to each recording session. For the HD recording sessions electrode impedances were measured immediately following GSN128 application and at the end of the recording sessions. Impedances were kept below 85 kΩ for the electrodes common to the LD and HD configurations and for most of the remaining electrodes. However, for the LD configuration it was not possible to get accurate impedance measurements from the EGI system with so few active electrodes (see Ferree et al., 2001). Since the active electrodes were hydrated and positioned on the scalp in exactly the same manner for both the LD and HD recordings, there is no reason for the impedances to be significantly different and all should be well below the 200 kΩ limit for accurate signal acquisition suggested by Ferree et al. (2001). Before starting both LD and HD recordings it was verified that the EEG signal from each electrode was not excessively noisy (which is often associated with high electrode impedances).

2.3. Data reduction

Each 1 min recording period was saved into a Netstation raw file calibrated in units of microvolts using the gains and zeros values measured at the beginning of each subject's recording session. These files were translated into Matlab (Mathworks Inc., Natick, MA) format for subsequent processing. First, each channel of EEG data was checked for clipped values greater than ±800 μV dynamic range which were automatically scored as bad. Then line noise was removed using a zero-phase 60 Hz notch filter in order to make it easier to visually inspect the data for artifacts. Finally the 6 active channels (LD) and all channels (HD) for each 1 min recording were manually scored for eye movement, blink, muscle (EMG) and motion artifacts. In order to verify that differences in scoring would not affect the results data from two of the participants were scored by a second human scorer. The average amount of data scored out by the two scorers across the 6 channels, all LD/HD recordings and two subjects was 3.5% with a single measure intraclass correlation of 0.84. The corresponding log-transformed power spectral density values (μV^2/Hz) in the 1–44 Hz band were −0.110 and −0.109, respectively, for the original and rescored data.

EEG data were analyzed following standard procedure in our laboratory (see Davidson et al., 2000b, for a review). Separate power spectral density estimates were made for each of the 6 active electrodes (referenced to Cz) for each 1 min recording period using Welch's method (Welch, 1967) applied to 1 s linearly detrended and Hanning windowed epochs of artifact-free data with 0.5 s of overlap. These raw power spectral density estimates at 1 Hz resolution were saved together with values averaged over selected bands. To normalize the data, all power density values were log-transformed (Davidson et al., 1990; Gasser et al., 1982). The log-transformed band means were averaged separately over the 3 eyes closed and 3 eyes open 1 min recording periods weighted by the number of artifact-free epochs of data in each period. The mean number of available epochs per channel across the 6 LD recording periods was 649 (range 584–691, SD = 41) compared to 651 (range 621–702, SD = 29) for the HD condition.

Participant 7 showed extremely large variation in muscle tension (EMG) signal between recording periods for both the LD and HD recordings. Since manual scoring would have removed most of the data, a regression method for correcting for this large EMG variation (Davidson et al., 2000c) was applied to the log-transformed EEG band means from each of this participant's 6 recording periods in order to remove the EMG effect. Separate regressions of log-transformed EEG band powers on the 70–80 Hz log-transformed band powers which are presumed to be exclusively myogenic in origin, were performed for each of the electrode sites and EEG bands. These regressions yielded residualized values which were used for participant 7.

Finally, for all participants, eyes closed and eyes open values were averaged with equal weighting for each of the 6 active electrodes and the averages across these electrodes were submitted to paired t tests for comparing the LD and HD results.

In order to detect possible electrolyte bridging Hjorth electrical distances were computed for each resting recording period using equation 4 from Tenke and Kayser (2001):

$$D_{i-j} = \frac{1}{T}\sum_{t=1}^{T}(P_{i-j}(t) - \overline{P_{i-j}(t)})^2 \quad (1)$$

where D_{i-j} and P_{i-j}, and $\overline{P_{i-j}}$ are the Hjorth electrical distance, the potential difference, and the mean potential difference, respectively, between electrodes i and j, and T is the time interval used. Thus the Hjorth electrical distance between two electrodes is simply the temporal variance of their difference potential. Tenke and Kayser (2001) worked with approximately 1 s of averaged EEG (i.e. ERP) data and suggested that their method might work with unaveraged data if it were detrended and filtered to remove individual amplifier drift and noise. For this study Hjorth electrical distances were computed by first bandpass filtering (0.25–20 Hz) all 60 s of data and then using the artifact-free segments from each recording period. There is no set threshold Hjorth electrical distance below which two electrodes would be considered as bridged. Tenke and Kayser (2001) reported Hjorth electrical distances between 0.054 and 0.140 μV^2 for presumed bridging due to excess electrolyte solution with the GSN128. However, they worked with averaged ERPs and were looking only for electrolyte bridges; here we want to detect possible electrolyte spreading in addition to bridging. A histogram of Hjorth electrical distances for the 8 participants in this study (Fig. 1a) showed a peak at 8 μV^2 with decreasing numbers until about 3 μV^2 where numbers began to increase again. Thus, for this study a threshold of 3 μV^2 was used and for a pair of electrodes to be designated as affected it was required that the Hjorth electrical distance remain under this threshold for all 6 recording periods.

An attempt was made to correct power values at any of the 6 common electrodes affected by bridging or electrolyte spreading during the HD recordings displayed in Fig. 2a. Raw EEG signals at the electrodes identified as bridged were estimated using the spherical spline interpolation method of Perrin et al. (1989, 1990). Spherical spline interpolation is an accepted method of replacing missing data by utilizing all electrodes that contain usable data, and its smoothed curvature produces better results than nearest-neighbor interpolation (Perrin et al., 1989, 1990; Soong et al., 1993; Fletcher et al., 1996). For these interpolations it

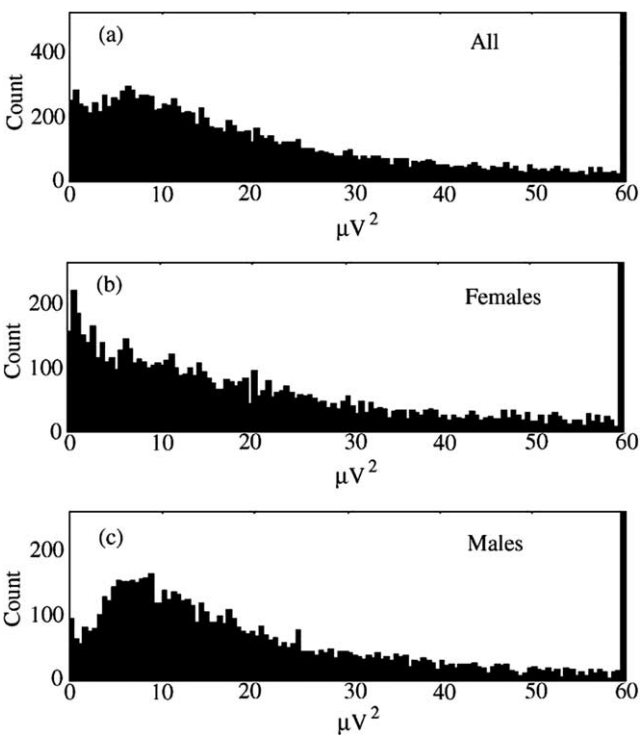

Fig. 1. Histograms of Hjorth electrical distances between neighboring electrodes. Bins are 0.5 μV^2 with counts shown on the vertical axis. Results from the 8 HD which followed the LD recordings are shown in (a), for the 4 female participants (b), and the 4 male participants (c).

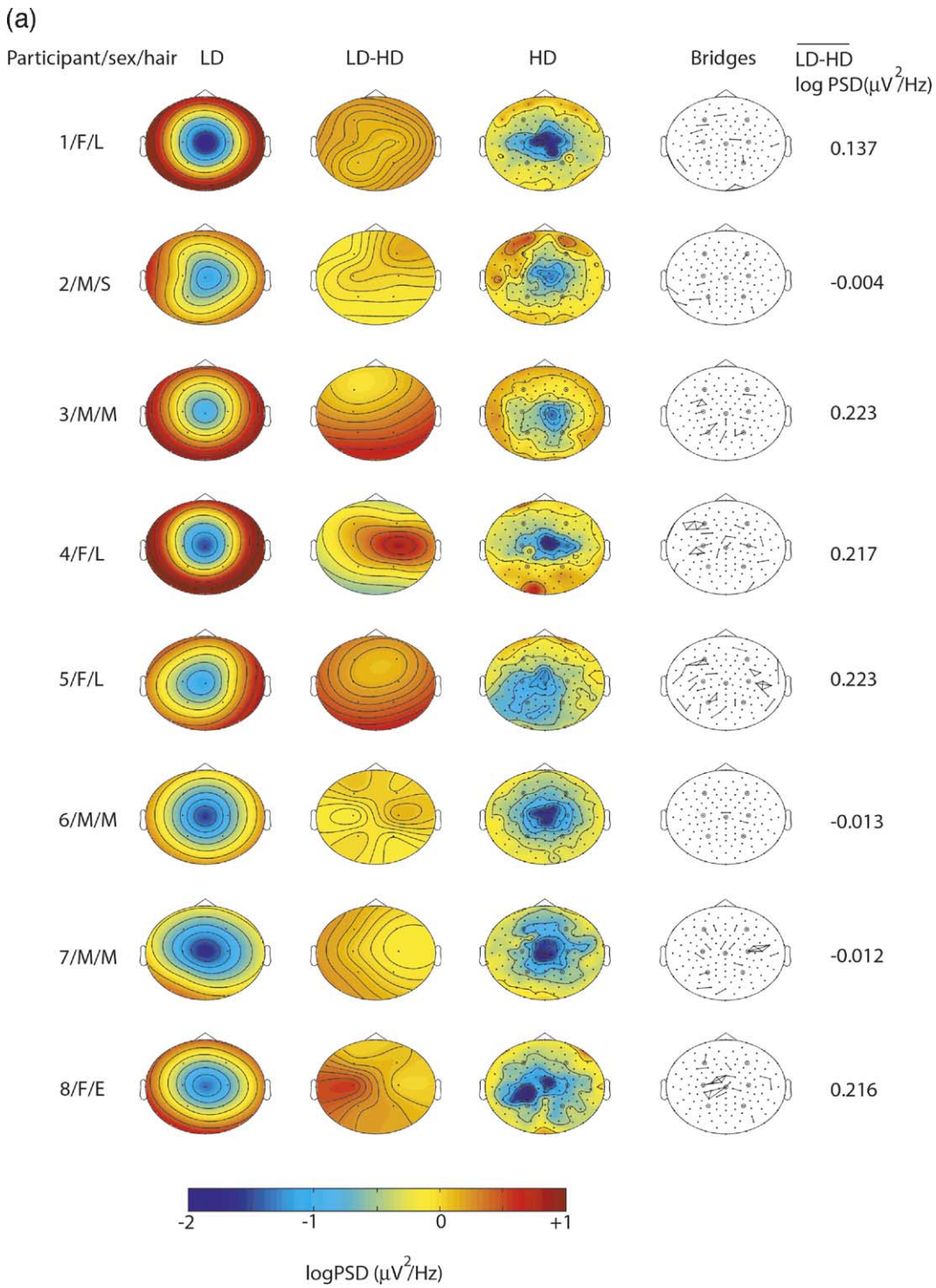

Fig. 2. Each row presents results for a single participant with number/sex/hair in first column, followed by two-dimensional maps of Cz-referenced mean log-transformed power spectral density PSD (μV^2/Hz) in the 1–44 Hz band for the LD recording periods, LD minus HD values at the same 6 electrodes, the HD maps for all 128 electrodes, and plots showing bridged electrodes in columns 2–5, respectively. Since Cz is a singularity in these maps ($\log 0 = -\infty$) the maps in the second column used the mean of the 4 electrodes nearest Cz in the HD map for the value at Cz. Bad channels in the HD maps in column 4 were interpolated using spherical splines (Perrin et al., 1989; Perrin et al., 1990). Bridges are shown for a Hjorth electrical distance threshold of 3 μV^2 calculated as described in text. The 6 active electrodes and Cz are marked by circles in the bridging maps. Column 6 shows the mean LD minus HD log-transformed PSD (μV^2/Hz) difference in the 1–44 Hz band for each participant. It should be noted that the LD maps in column two represent a sparse sampling and are presented as a comparison for the production of the difference maps shown in column 3. A qualitative coding of hair length for each participant is coded as the last item in column one as follows: L, shoulder hair length or greater; E, hair length from top of head to ears or covering ears; M, hair length greater than average electrode separation on the GSN128; S, hair length less than average electrode separation on the GSN128. Results for 8 participants with LD followed by HD recordings are shown in (a), and results for a subset of participants with HD followed by LD recordings are shown in (b).

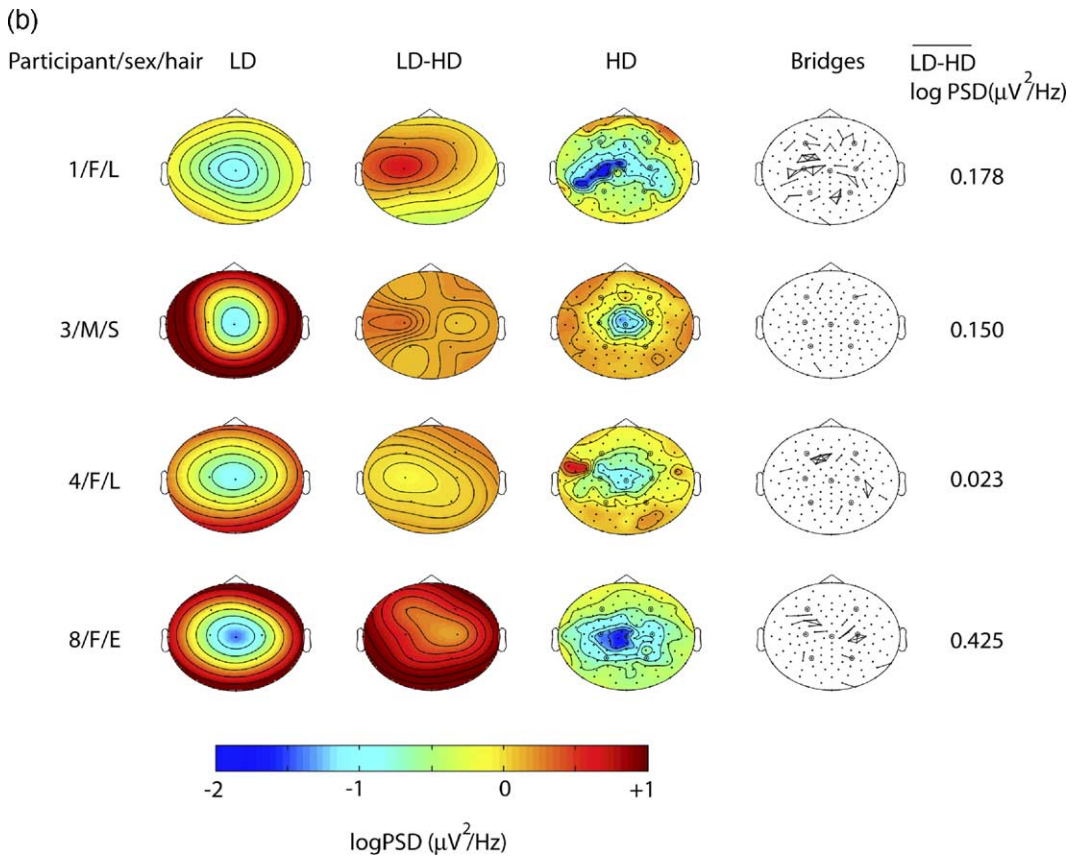

Fig. 2. *(continued)*

was still ensured that at least one nearest neighbor electrode with good data values existed. The interpolated raw EEG signals at these bridged electrodes were input to the power spectral program and the mean log-transformed wide (1–44 Hz) power values were computed for 7 of the participants (participant 7 was dropped because of the EMG problem) as described above. Thus for each electrode identified as being affected by bridging there existed two power values one estimated from original affected signal and one from signal interpolated using unaffected electrodes.

This spherical spline interpolation method of power correction was also tested on data from 17 (12 female) undergraduates at the University of Wisconsin-Madison selected from a previously-collected longitudinal data set (Silva et al., 2002; Jackson et al., 2000). Ages ranged between 18 and 27 (mean = 19, SD = 2). The only selection criterion was that they possess at least one bridged pair of electrodes (mean = 1.59, SD = 0.71) in the left-frontal quadrant of the GSN128 (left of mid-line, anterior to the left preauricular point.

The method of applying the GSN128 was identical to that described above for the HD recordings except that a higher concentration of potassium chloride (~24 g/l) was used at the time these data were recorded in an attempt to lower scalp impedances. Eight 1 min resting EEG recordings were collected using the same sampling rate and hardware filter settings but at 12 bits of precision using older EGI amplifiers and Netstation 1.0 software. This lower precision required a clipped value threshold set to the ±200 μV dynamic range of this recording system. One second epochs from a variable number of 1 min recording periods (mean = 2.71, SD = 1.49) for each participant were used in analyses based on whether or not bridged sites were detected in the left-frontal quadrant. Hjorth electrical distances were computed using eq. (1) with $T = 50$ s and a threshold for bridging of 1 μV^2. Input was the 20 Hz low-passed filtered and detrended data before artifact removal. Mean log-transformed alpha band power spectral values of the Cz referenced data were computed using all artifact-free 1 s epochs (0.5 s overlap) from each participant's selected one-minute recording periods.

Raw EEG signals at the electrodes identified as bridged were estimated using the spherical spline interpolation method of Perrin et al. (1989, 1990) as described above. The interpolated raw EEG signals at these bridged electrodes were input to the power spectral program and the mean log-transformed alpha power values were computed for each subject using the same selected recording periods (i.e. the same artifact-free 1 s epochs). Again, for each electrode identified as being affected by bridging there existed two

Table 1
Paired t tests between LD followed by HD measurements (log-transformed power values (μV^2/Hz)) for Wide band 1–44 Hz and for the various sub-bands

Band	Mean LD (SE)	Mean HD (SE)	LD-HD	t	P (two-tailed)	Effect size
Wide: 1–44 Hz	−0.425 (0.083)	−0.550 (0.063)	0.125	3.06	0.019	0.60
Delta: 1–4 Hz	0.122 (0.051)	−0.052 (0.027)	0.174	4.74	0.003	1.49
Theta: 4–8 Hz	−0.263 (0.081)	−0.406 (0.046)	0.143	3.26	0.014	0.76
Alpha: 8–13 Hz	−0.183 (0.140)	−0.251 (0.110)	0.067	1.38	0.211	0.19
Beta-1: 13–20 Hz	−0.614 (0.096)	−0.717 (0.092)	0.097	2.13	0.052	0.39
Beta-2: 20–33 Hz	−0.848 (0.104)	−1.001 (0.121)	0.153	2.87	0.025	0.48
Gamma-1: 36–44 Hz	−1.394 (0.101)	−1.557 (0.113)	0.163	3.18	0.016	0.53

For all tests the number of observations, $n = 8$ and degrees of freedom, df = 7.

power values: one estimated from original affected signal and one from signal interpolated using unaffected electrodes.

3. Results

Means over the six 1 min recording periods of the log-transformed mean power spectral density for the wide band (1–44 Hz) and for delta (1–4 Hz), theta (4–8 Hz), alpha (8–13 Hz), beta-1 (13–20 Hz), beta-2 (20–33 Hz) and gamma-1 (36–44 Hz) bands were submitted to paired t tests to assess differences between the LD and HD conditions. The mean LD and HD electrode values for the 6 active channels from each of the participants served as an observation. Table 1 shows the detailed output from the paired t tests for the 8 participants tested in the LD/HD order and the counterbalanced results for the subset of 4 participants with reversed order (LD/HD) measurements are in Table 2. Powers for HD electrode measurements were significantly smaller than the LD values irrespective of the counterbalanced order in the wide band and in most of the sub-bands. Cohen's effect size (Cohen, 1998) for repeated measures was computed using original standard deviations rather than the paired t test value in order to avoid overestimation (Dunlap et al., 1996). These effect sizes are listed in the last column of Tables 1 and 2 and ranged from small (≤ 0.2) for the alpha band to considerably over the large (0.8) threshold for the delta band.

Two-dimensional maps illustrating the power differences between the LD and HD recordings for the 8 participants recorded in the LD/HD order are shown in Fig. 2a and for the subset of 4 participants with HD/LD recording orders in Fig. 2b. Mean power maps for the LD recordings are shown in the second column, LD minus HD values at the 6 LD electrodes in the third column and the HD map for all 128 electrodes in the 4th column. It should be noted that the LD maps in column two represent a sparse sampling and are presented as a comparison for the production of the difference maps shown in column 3. A qualitative assessment of hair length is included as the last item in column one. For the LD/HD ordering participants 3, 4, 5 and 8 showed the largest differences between LD and HD powers along with the greatest number of bridges. Three of these 4 were females with hair longer than any of the males and participant 3 had the longest hair of the males. In fact, for the 8 participants illustrated in Fig. 2a, there were significantly more bridged electrode pairs observed in the female participants (mean = 24.5, SD = 9.5) than male participants (mean = 10.2, SD = 7.1) (unpaired $t = -2.39$, df = 6, $P < 0.03$). Fig. 2b shows the analogous results for participants 1, 3, 4 and 8 recorded in the HD/LD order. Participants 1 and 8 showed bridging and power decrement patterns similar to those of Fig. 2a while 3 and 4 showed fewer bridges and smaller power decrements.

Participants 4 and 8 showed particularly large power decreases for the LD/HD recording order (Fig. 2a) at C4 and C3, respectively, where there were nearly continuous

Table 2
Counterbalanced measurements for participants 1/F, 3/M, 4/F and 8/F

Band	Mean LD (SE)	Mean HD (SE)	LD-HD	t	P (two-tailed)	Effect size
Wide: 1–44 Hz	−0.299 (0.097)	−0.511 (0.119)	0.212	4.18	0.025	0.98
Delta: 1–4 Hz	0.200 (0.014)	0.010 (0.046)	0.190	5.33	0.013	2.78
Theta: 4–8 Hz	−0.059 (0.100)	−0.312 (0.121)	0.253	4.77	0.017	1.14
Alpha: 8–13 Hz	0.021 (0.170)	−0.170 (0.199)	0.190	4.51	0.020	0.51
Beta-1: 13–20 Hz	−0.518 (0.151)	−0.729 (0.163)	0.211	6.18	0.009	0.67
Beta-2: 20–33 Hz	−0.857 (0.163)	−1.088 (0.183)	0.231	5.24	0.014	0.66
Gamma-1: 36–44 Hz	−1.424 (0.077)	−1.601 (0.132)	0.177	2.81	0.067	1.28

For all tests the number of observations, $n = 4$ and degrees of freedom, df = 3.

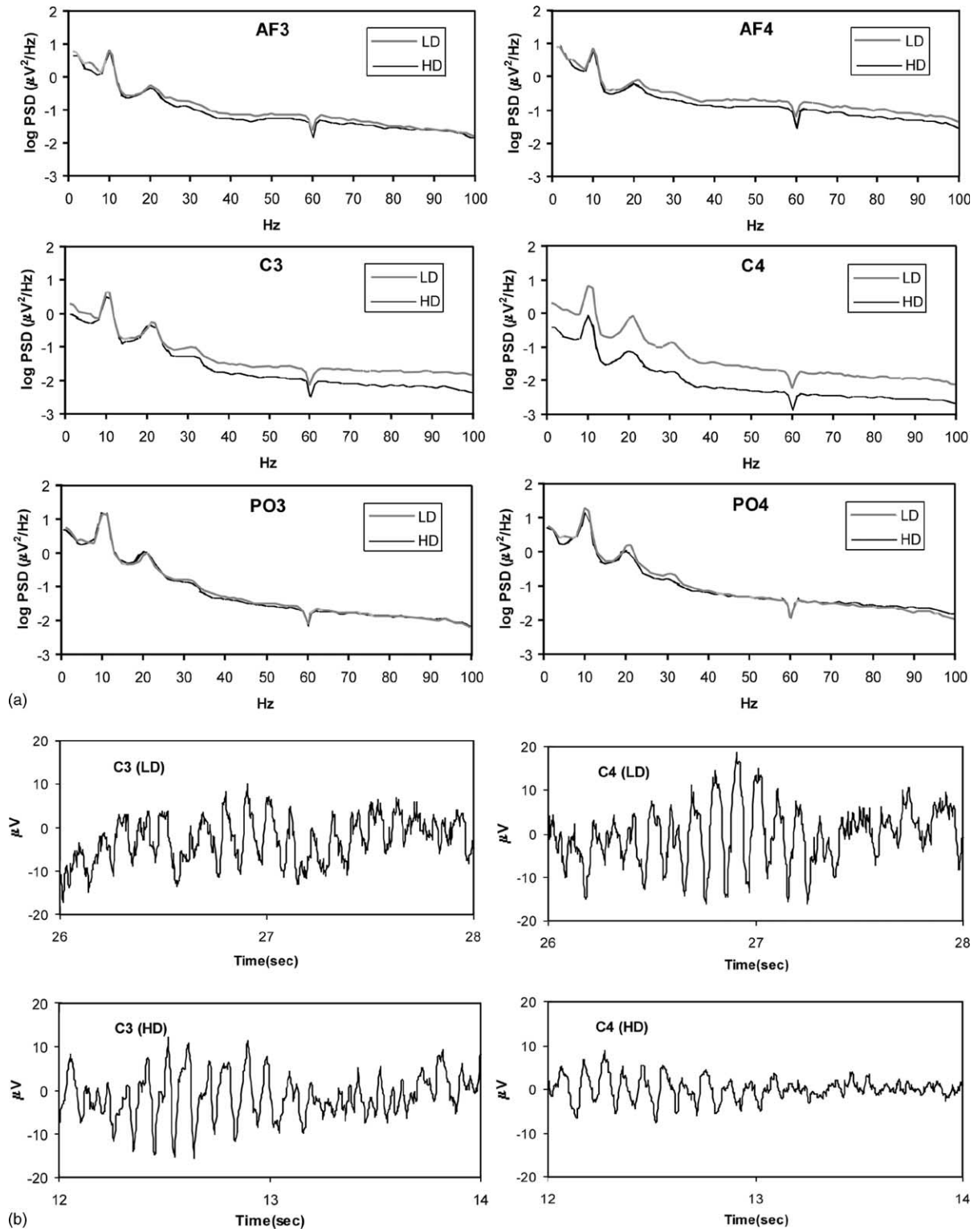

Fig. 3. Cz referenced power spectra for participant 4 are shown in (a). Log-transformed power values (μV^2/Hz) were computed as described in the text using 1 Hz bands with LD and HD measurements plotted with light and dark lines, respectively. The 6 plots are arranged according to relative electrode position with frontal sites located in the top row. Panel (b) shows 2 s of raw data from homologous central electrodes C3/4 illustrating the decrement in voltage recorded at C4 during the HD recording.

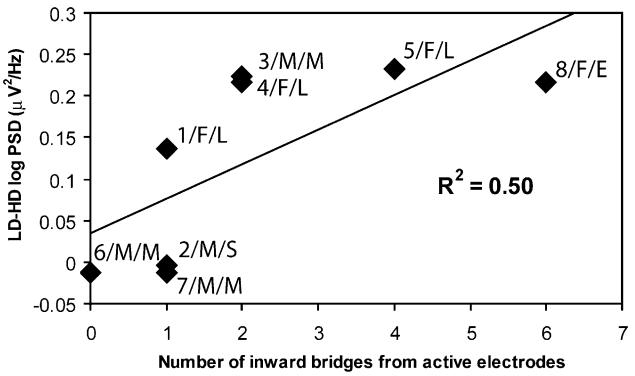

Fig. 4. Regression of LD-HD power differences (LD/HD recording order) on the number of bridges extending inward towards Cz as illustrated in column 4 of Fig. 2a ($r = 0.70$, n = 8, $P = 0.05$). Participant number/sex/hair is shown next to each data point.

bridging paths between these electrodes and Cz. The power spectra for participant 4 (LD/HD recording order, Fig. 2a) at the 6 LD sites are shown in Fig. 3a arranged according to relative electrode position. Large power decreases for the HD recording at C4 occurred throughout the frequency range while the LD/HD differences at the other electrodes were relatively small. Fig. 3b shows representative simultaneous 2 s sections from the first eyes closed LD and HD EEG recordings at homologous sites C3/4 for participant 4. The diminished signal at C4 for the HD recording is obvious and appears to be due to a straightforward decrease in signal amplitude. The corresponding power spectrum for C4 shown in Fig. 3a shows a quite uniform decrease in power at all frequencies consistent with the amplitude decrease illustrated in Fig. 3b which is also apparent when the entire artifact-free EEG record is plotted.

In order to test for a relation between the decrease in HD power values at the 6 LD electrode sites, the power differences listed in column 6 of Fig. 2a were regressed on the number of electrode bridges illustrated in column 5 which extended inward from any of the 6 active electrodes towards the lower powers observed near the Cz reference. The scatter plot and regression line are shown in Fig. 4 ($r = 0.70, n = 8$, $P = 0.05$) with each point labeled with participant number, sex, and qualitative hair length. This is a rather crude model since it ignores possible bridging from the active electrodes into other low power areas. However, it serves to illustrate that the observed power decrease for these particular 6 electrode sites during the HD recordings appears to be due to a preponderance of bridging into low power areas. The network of bridging extending from participant 7's C4 electrode outward away from Cz is a good example of increased power for the HD recording. Power contours near this electrode (4th column in Fig. 2a) show high-power values extending to it from the lower right with low-power values extending outward to the electrode at the far end of the bridging network as expected from the averaging effect of the bridging (resulting in the negative value at C4 in the LD minus HD difference map in the third column).

Bridges detected by the Netstation 3.0 in real time during collection of the 4 counterbalanced HD/LD ordered EEG recordings were compared to those detected by the off-line method described in this paper with the threshold set to 1 μV^2 in order to minimize differences between the two methods. Overall, Netstation 3.0 detected fewer bridges for the HD recordings of the counterbalanced sessions (10 of 19 plus 7 not in group of 19; 1 of 1 plus 1 additional; 6 of 10 plus 3 not in group of 10; and 0 of 3 for participants 1/F/L, 3/M/M, 4/F/L and 8/F/E, respectively) than the off-line bridge detection described here. Although the agreement between the two methods was not particularly good this real-time bridge detection incorporated into Netstation could potentially help reduce bridging prior to beginning an EEG recording session.

Using spherical spline interpolation to correct electrode power values affected by bridging reduced the difference between the mean LD and HD powers for the 6 electrodes common to both the recordings by increasing the mean log-transformed wide (1–44 Hz) power for the HD recordings (mean = −0.51, SD = 0.14 compared to mean = −0.48, SD = 0.16 using the interpolated values; $t = 1.38$, df = 6, $P = 0.21$). However, the interpolated values were not significantly different from the original bridged values and the difference between the mean LD and HD powers for the 6 common electrodes remained significant ($t = 2.92$, df = 6, $P = 0.03$). For the larger number of participants in the second test, log-transformed alpha power increased significantly at bridged sites (mean = 0.28, SD = 0.32) when data were interpolated as compared to original data from the same bridged sites (mean = 0.23, SD = 0.34, t = 4.02, df = 16, $P = 0.001$). These findings demonstrate the potential of spherical spline interpolation as a practical method for correcting power values affected by electrolyte spreading. However, more work needs to be done to test whether this correction method improves the reliability of asymmetry scores.

4. Discussion

A significant decrease in HD power values at the 6 chosen electrodes (AF3/4, C3/4, PO3/4) was observed for LD and HD EEG measurements with the GSN128 (Tables 1 and 2). The LD minus HD mean difference for the wide band shown in Table 1 represents approximately a 13% decrease in signal strength and thus a corresponding decrease in signal-to-noise ratio which agrees qualitatively with previous work using the GSN128 (Kayser et al., 2000). Debener et al. (2002) reported that the use of a GSN does not necessarily result in a lower signal-to-noise ratio. However, in response to this paper, Kayser et al. (2003) point out that Debener et al. (2002) used data averaged across multiple sites and the premise that reliability analyses

are sufficient estimates of ERP signal-to-noise ratios. The work presented here supports the results of Kayser et al. (2000) that a direct comparison of HD and LD data indicates a lower signal-to-noise ratio for the GSN HD recordings.

Furthermore, a significant relation was found between the observed power decrease and an estimate of overall electrolyte spreading/bridging from these electrodes towards the smaller powers observed near the Cz reference (i.e. spatial blurring towards Cz) for the 8 LD/HD recordings (Fig. 4). The association between these two conditions provided evidence for the HD power decrease being caused by electrolyte bridging and – due to the counterbalancing strategy used in the present study – against it being due to source differences or changes in functional brain states between the low- and high-density recording conditions. Patterns of bridging (Fig. 2a,b) were generally consistent with sloping areas of the head where electrolyte would naturally flow or be wicked by hairs. It should be noted that for the HD followed the LD recordings (Table 1 and Fig. 2a) any residual (not yet evaporated) electrolyte left near the 6 active sites could potentially have increased spreading and contributed to the HD results. However, this effect should not be greater than lifting and moving the GSN128 during an initial application in order to get a better placement of the electrodes. In addition, counterbalancing the subset of 4 participants with reversed order HD followed by LD recordings also showed decreased power for the HD recordings.

The fact that a mean power decrement was observed may be due to the predominance of bridging effects towards the reference at Cz from the chosen 6 electrodes. For LD EEG recordings each electrode is relatively isolated so electrolyte spreading at an electrode effectively changes the area over which its potential is measured but without significantly affecting neighboring electrodes. However, for HD recordings it is relatively easy for electrolyte spreading to create a nearly continuous path including several electrodes. The saline solution used with the GSN128 flows easier than electrolyte gels and the sponge electrodes are more open than the electrode housings used in cap systems. The large power decrease at electrode C4 for participant 4 (Figs. 2a and 3) was associated with a surface path between C4 and Cz consisting of scalp in parallel with a nearly continuous layer of the much higher conductivity electrolyte. Such a result seriously blurred the voltages between C4 and Cz and could occur in a HD recording using any electrode system that allowed a similar pattern of electrolyte spreading.

No attempt was made to distinguish between electrolyte spreading and bridging since the end result is the same – a diminished voltage difference between the affected electrodes. Hjorth electrical distances between electrodes were used to estimate these voltage differences and provide circumstantial evidence for bridging. Although it is theoretically possible for a zero Hjorth electrical distance to exist between two unbridged electrodes for a single strong source this condition is not likely to last for the entire period over which the Hjorth electrical distances were estimated. A distribution of Hjorth electrical distances similar to that illustrated in Fig. 1c was expected for HD recordings where electrolyte spreading/bridging was relatively subdued.

It is suggested that the high-density electrode array combined with the effects of electrolyte spreading may act as a spatial low pass (high cut) filter with properties that vary depending on the local distribution of electrodes and electrolyte spreading. Tables 1 and 2 show for the data presented here that the greatest effect sizes occur in the delta and theta bands which Nunez et al. (2001) describe for the relaxed waking state as having spatial spectra more dominant at higher spatial frequencies while alpha rhythms which show smaller effect sizes have substantial power at low spatial frequencies. An interesting area for future research would be to incorporate EEG electrodes into a suitably accurate head model (e.g. finite element model) and directly test the effects of electrode number, size and electrolyte spreading on the signals of various spatial frequencies.

Detecting and correcting for power decrements due to electrolyte spreading or bridging is particularly important for estimating asymmetry scores from relaxed EEG recordings where consistent bridging effects in one hemisphere can easily skew the estimate. Ideally, electrolyte bridges should be detected and removed before recording begins. The on-line bridge detection software (Electrical Geodesics Inc., 2003) showed potential for accomplishing this goal and similar programs could be developed for other systems. For off-line identification of affected electrodes Hjorth electrical distances combined with scalp maps of power appear to be feasible although additional research on identifying anomalous Hjorth electrical distances which represent true electrolyte spreading effects would be useful. This strategy is similar to the plotting of median maximum absolute potentials versus polar angle from Cz already proposed by Junghöfer et al. (2000) who also worked with EEG data recorded using the GSN128.

Some success was achieved by using a fixed threshold for mapping bridges and spherical spline interpolation to correct power values at affected electrodes. However, more work is required to assess these corrections and determine whether they improve estimates of asymmetry scores. Future work will examine distributions of Hjorth electrical distances and attempt to determine variable (perhaps based on direction) thresholds for anomalously low values.

A more definitive assessment of affected electrodes would be very useful for correcting these effects while maintaining maximal spatial resolution. Limits on the total number of affected electrodes that can be usefully interpolated still need to be determined.

There were significantly more bridged electrode pairs observed in the female participants than male participants displayed in Fig. 2a. The Hjorth electrical distance histograms for the male and female participants (Fig. 1b,c) also illustrate this difference with the peak at a smaller

electrical distance for the female participants. It is also obvious from the regression plot (Fig. 4) that gender/hair length appears to be a factor in that relation. These results strongly imply that hair length may be a possible factor for electrolyte spreading and agree with the EGI assessment from their on-line bridge detection software (Electrical Geodesics Inc., 2003) that bridges are caused by electrodes that are physically touching or are sitting on a mat of hair which allows a continuous bridge of electrolyte to exist between them. Given these results a more detailed study of the role of hair length on electrolyte spreading is probably warranted for this and other high-density EEG recording systems.

The results presented here suggest that truly realistic head models for high-density EEG recordings need to continue outward beyond the surface of the scalp to include the electrodes and electrolyte. Such models would help quantify electrolyte spreading effects and might reveal whether high-density EEG recordings enable detection of high spatial frequency signals while somewhat diminishing their amplitudes.

Acknowledgements

This work was supported by NIMH grants R01-MH40747, R37-MH43454, P50-MH52354 to RJD. DAP was supported by grants from the Swiss National Research Foundation (81ZH-52864) and 'Holderbank'-Stiftung zur Förderung der wissenschaftlichen Fortbildung

References

Cohen J. Statistical power analysis for the behavioral sciences, 2nd ed. Hillsdale, NJ: Lawrence Erlbaum; 1998.

Davidson RJ. EEG measures of cerebral asymmetry: conceptual and methodological issues. Int J Neurosci 1988;39:71–89.

Davidson RJ, Chapman JP, Chapman LJ, Henriques JB. Asymmetrical brain electrical activity discriminates between psychometrically-matched verbal and spatial tasks. Psychophysiology 1990;47:85–95.

Davidson RJ, Jackson DC, Kalin NH. Emotion, plasticity, context, and regulation: Perspectives from affective neuroscience. Psychol Bull 2000a;126:890–909.

Davidson RJ, Jackson DC, Larson CL. Human electroencephalography. In: Cacioppo JT, Tassinary LG, Bernston GG, editors. Handbook of psychophysiology, 2nd ed. Cambridge, UK: Cambridge University Press; 2000b. p. 27–56.

Davidson RJ, Marshall JR, Tomarken AJ, Henriques JB. While a phobic waits: regional brain electrical and autonomic activity in social phobics during anticipation of public speaking. Biol Psychiatry 2000c;47:85–95.

Dunlap WP, Cortina JM, Vaslow JB, Burke MJ. Meta-analysis of experiments with matched groups or repeated measures designs. Psychol Methods 1996;1:170–7.

Debener S, Kranzioch C, Herrmann CS, Engal AK. Auditory novelty oddball allows reliable distinction of top-down and bottom-up processes of attention. Int J Psychophysiol 2002;46:77–84.

Electrical Geodesics Inc., On-line detection of electrolyte bridges. EGI Newslett 2003;7(1):1.

Ferree TC, Tucker DM. Development of high-resolution EEG devices. Int J Bioelectromagn 1999;1(1):4–10.

Ferree TC, Luu P, Russell GS, Tucker DM. Scalp electrode impedance, infection risk, and EEG data quality. Clin Neurophysiol 2001;112:536–44.

Fisher RA. On the probable error of a coefficient of correlation deduced from a small sample. Metron 1921;1:3–32.

Fletcher EM, Kussmaul CL, Mangun GR. Estimation of interpolation errors in scalp topographic mapping. Electroenceph clin Neurophysiol 1996;98:422–34.

Gasser T, Bacher P, Mocks J. Transformations toward the normal distribution of broad band spectral parameters of the EEG. Electroenceph clin Neurophysiol 1982;53:119–24.

Jackson DC, Burghy CA, Hanna AJ, Larson CL, Davidson RJ. Resting frontal and anterior temporal EEG asymmetry predicts ability to regulate negative emotion. Psychophysiology 2000;37:S50.

Junghöfer M, Elbert T, Tucker DM, Rockstroh B. Statistical control of artifacts in dense array EEG/MEG studies. Psychophysiology 2000;37:523–32.

Kayser J, Tenke CE, Bhattacharya N, Stuart BK, Bruder GE. A direct comparison of Geodesic Sensor Net (128-channel) and conventional (30-channel) ERPs in tonal and phonetic oddball tasks. Psychophysiology 2000;37:S17. Paper and animations available at URL http://psychophysiology.cpmc.columbia.edu/DEA2000.html.

Kayser J, Tenke CE, Bruder GE. Letter to the editor: evaluating the quality of ERP measures across recording systems: a commentary on Debener et al. (2002). Int J Psychophysiol 2003;48:350.

Lantz G, Grave de Peralta R, Spinelli L, Seeck M, Michel CM. Epileptic source localization with high density EEG: how many electrodes are needed? Clin Neurophysiol 2003;114:63–9.

Luu P, Ferree TC. Determination of the Geodesic sensor net's average electrode positions and their 10–10 international equivalents. Technical Note, Electrical Geodesics, Inc. Electrical Geodesics Inc; 2000.

Nunez PL, Brett M, Silberstein RB. Spatial-temporal structures of human alpha rhythms: theory, microcurrent sources, multiscale measurements, and global binding of local networks. Hum Brain Mapp 2001;13:1125–64.

Perrin F, Pernier J, Bertrand O, Echallier JF. Spherical splines for scalp potential and current density mapping. Electroenceph clin Neurophysiol 1989;72:184–7.

Perrin F, Pernier J, Bertrand O, Echallier JF. Corrigenda: EEG 02274. Electroenceph clin Neurophysiol 1990;76:565.

Silva JR, Pizzagalli DA, Larson CL, Jackson DC, Davidson RJ. Frontal brain asymmetry in restrained eaters. J Abnorm Psychol 2002;111(4):676–81.

Soong ACK, Lind JC, Shaw GR, Koles ZJ. Systematic comparisons of interpolation techniques in topographic brain mapping. Electroenceph clin Neurophysiol 1993;87:185–95.

Spitzer AR, Cohen LG, Fabrikant J, Hallett M. A method for determining optimal interelectrode spacing for cerebral topographic mapping. Electroenceph clin Neurophysiol 1989;72:355–61.

Srinivasan R, Tucker DM, Murias M. Estimating the spatial nyquist of the human EEG. Behav Res Methods Instrum Comput 1998;30(1):8–19.

Tenke CE, Kayser J. A convenient method for detecting electrolyte bridges in multichannel electroencephalogram and event related potential recordings. Clin Neurophysiol 2001;112:545–50.

Tomarken AJ, Davidson RJ, Wheeler R, Kinney L. Psychometric properties of resting anterior EEG asymmetry: temporal stability and internal consistency. Psychophysiology 1992;29:576–92.

Tucker DM. Spatial sampling of head electrical fields: the geodetic sensor net. Electroenceph clin Neurophysiol 1993;87:154–63.

Welch PD. The use of fast Fourier transform for the estimation of power spectra: a method based on time averaging over short, modified periodograms. IEEE Trans Audio Electroacoust 1967;15:70–3.